

# **Numerical studies of hydrate crystal growth during $CO_2$ sequestration**

Dongxiao Zhang, Peter C. Lichtner, Qinjun Kang, and Ioannis N. Tsimpanogiannis,

Hydrology, Geochemistry, and Geology Group

Los Alamos National Laboratory, Los Alamos, NM 87545.

Since  $CO_2$  was identified as a major contributor to the global warming problem, a large number of studies have been undertaken to investigate possible solutions of removing/disposing the produced  $CO_2$  while attempting to satisfy our continuously increasing needs for energy consumption. Methods considered include oceanic disposal, injection into oil reservoirs/saline aquifers, chemical capture, etc. During the disposal process, if the prevailing conditions include high pressures and/or low temperatures and water is present, the formation of hydrate (a crystalline structure made up of hydrogen-bonded water molecules stabilized by gas) is possible. As hydrate is formed, changes in porosity/permeability of the medium used for disposal will occur, affecting to some degree, yet to be identified, the disposal process. Compared to advances made in hydrate thermodynamics, the formation and decomposition kinetics of hydrate is less understood. A better knowledge of kinetics would provide a more accurate estimate of the hydrate formation/decomposition rate. It has been theoretically demonstrated and experimentally observed that hydrate formation is not restricted to a thin layer close to the gas-liquid interface but can occur anywhere in the liquid water phase if the solution is supersaturated. In this work, we have used the lattice Boltzmann (LB) method, to numerically simulate hydrate formation from a supersaturated solution. We performed a set of sensitivity tests varying the Damkohler number and saturation using a first-order kinetic rate law and examined the effects of these parameters on the patterns of hydrate formation.

## Introduction

Since  $CO_2$  was identified as a major contributor to the global warming problem, a large number of studies have been undertaken to investigate possible solutions of removing/disposing the produced  $CO_2$  while attempting to satisfy our continuously increasing needs for energy consumption. Methods considered include oceanic disposal, injection into oil reservoirs/saline aquifers, chemical capture, etc. During the disposal process, if the prevailing conditions include high pressures and/or low temperatures and water is present, the formation of hydrate (a crystalline structure made up of hydrogen-bonded water molecules stabilized by gas) is possible. As hydrate is formed, changes in porosity/permeability of the medium used for disposal will occur, affecting to some degree, yet to be identified, the disposal process. Compared to advances made in hydrate thermodynamics, the formation and decomposition kinetics of hydrate is less understood [1]. A better knowledge of kinetics would provide a more accurate estimate of the hydrate formation/decomposition rate.

Pore-scale study is very important in the study of gas hydrates, because it can provide detailed process and mechanism of hydrate formation/dissociation; can identify key parameters and processes that control hydrate formation/dissociation; can investigate the impact of hydrate formation/dissociation on porosity, permeability, and other properties of the porous medium; and it can study the effects of pore-scale structures and processes on macroscopic constitutive relations. When combined with upscaling techniques, pore-scale study can provide effective diffusivity, porosity-permeability, relative permeability and other constitutive relations needed for continuum modeling. However, there is no prior numerical work on pore-scale study of hydrate growth. There exist some related numerical studies on crystal growth, including macroscopic approach, which solves continuum diffusion equation coupled with moving boundary conditions [2]; microscopic approaches, such as diffusion limited aggregation (DLA) and multi-particle DLA, using Monte Carlo method to track the individual growth units [3]; and Lattice Boltzmann method with enhanced collisions and phase-field method [4].

In this study, we aim to develop a pore-scale numerical method for hydrate formation that is efficient, grid-effects free, capable of handling complex geometries (boundaries), and able to simulate anisotropic growth. the lattice Boltzmann (LB) method with a Bhatnagar-Gross-Krook (BGK) collision operator is a good candidate for these purposes. Unlike conventional numerical methods based on macroscopic continuum equations, this method is based on microscopic models and mesoscopic kinetic equations [5]. Therefore, it can model problems where both macroscopic and microscopic scales are important and it is particularly suitable for solving non-equilibrium problems, such as liquid/solid phase transition. Since its appearance, it has been successful for fluid flow applications involving interfacial dynamics and complex boundaries. It is also a powerful tool for modeling physical phenomena that are

not easily described by macroscopic equations. In addition, its algorithm is fully parallelizable, and it is easy to implement boundary conditions in this method.

## Numerical method

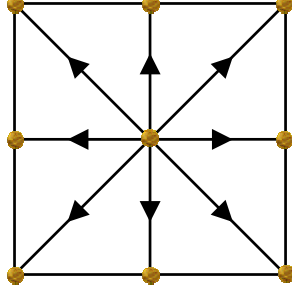


Figure 1: Schematic illustration of the two-dimensional, nine-speed lattices.

In the LB method, the primitive variable is the particle distribution function, which is defined for each lattice vector  $\mathbf{e}_i$  at each site  $\mathbf{x}$ , as shown in figure 1. In order to capture fluid dynamics, the distribution function is manipulated by a streaming-collision process for each time-step, as described by the following evolution equation:

$$f_i(\mathbf{x} + \mathbf{e}_i \delta_t, t + \delta_t) = f_i(\mathbf{x}, t) - \frac{f_i(\mathbf{x}, t) - f_i^{eq}(\rho, \mathbf{u})}{\tau}. \quad (1)$$

Using Chapman-Enskog multiscale expansion technique, we can prove that this evolution equation recovers the correct continuity and momentum equations at the Navier-Stokes level.

$$\frac{\partial \rho}{\partial t} + \bar{\nabla} \cdot (\rho \mathbf{u}) = 0, \quad (2)$$

$$\frac{\partial (\rho \mathbf{u})}{\partial t} + \bar{\nabla} \cdot (\rho \mathbf{u} \mathbf{u}) = -\bar{\nabla} p + \bar{\nabla} \cdot [\mu (\bar{\nabla} \mathbf{u} + \mathbf{u} \bar{\nabla})], \quad (3)$$

where density is defined by  $\rho = \sum_i f_i$ , and velocity is given by  $\rho \mathbf{u} = \sum_i \mathbf{e}_i f_i$ . The pressure is given by

an equation of state  $p = \frac{1}{3} \rho$ , and the viscosity is related to the relaxation time by  $\mu = \frac{\rho}{3} (\tau - 0.5)$ .

Similarly, we can introduce another particle distribution function to simulate the solute transport and its evolution equation can be proved to recover the convection-diffusion equation.

Since its appearance, the LB method has been successfully applied to studying a variety of flow and transport phenomena such as single or multiphase flow in porous media, turbulence, particles

suspended in fluids, liquid/solid phase transition. We have developed a LB model for simulating dissolution and precipitation in porous media [6-8], a parallel code for multiphase/multicomponent flow [9-11], and a LB model for flow and solute transport in fractured porous media [12,13]. Based on these models, we have developed a LB model for simulating hydrate formation [14]. It has been theoretically demonstrated and experimentally observed that hydrate formation is not restricted to a thin layer close to the gas-liquid interface but can occur anywhere in the liquid water phase if the solution is supersaturated [15]. Even though there is not a unified hydrate kinetics model yet, it is important to perform a set of sensitivity studies on the control parameters based on the existing kinetics models. A typical kinetic model for hydrate formation was proposed by Englezos et al [16].

$$\left(\frac{dn}{dt}\right)_p = k^* A_p (f_b - f_{eq}), \quad (4)$$

where  $\left(\frac{dn}{dt}\right)_p$  is the rate of growth per particle. The quantity of  $f_b - f_{eq}$  is the difference in the fugacity of the dissolved gas and its fugacity at the three-phase equilibrium. It defines the overall driving force.  $A_p$  is the surface area of each particle.  $k^*$  is the combined rate constant for the diffusion and adsorption processes and is the only adjustable parameter in this model and to be determined from experimental data on formation kinetics of hydrates. In this study, for simplicity and generality, we consider the following first-order kinetic reaction model at the liquid-hydrate interface,

$$D \frac{\partial C}{\partial n} = k_r (C - C_s), \quad (5)$$

which is slightly different from Englezo's kinetic model. Here the driving force is the difference in concentration and  $k_r$  is the reaction rate constant or consumption rate constant of the solute. The effect of temperature and pressure can be taken into account through  $D$  and  $k_r$ . We track the hydrate mass accumulation in each control volume at the interface. When this mass doubles, one of the neighboring liquid nodes is chosen randomly to become a hydrate node.

### Simulation setup (no flow)

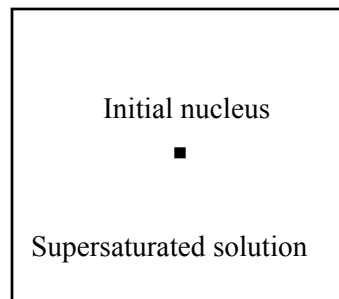


Figure 2: Simulation setup.

Figure 2 shows the simulation setup. The size of the cavity is 200×200. Initially, the domain is filled with supersaturated solution. At time zero, a stable nucleus is introduced at the center of the domain. Hydrates begin to grow subsequently. Dimensional analysis suggests two dimensionless parameters that control the process: saturation ( $\psi = \frac{C_0}{C_s}$ ) and Damkohler number ( $Da$ , the ratio of reaction to diffusion). Figure 3 shows Hydrate structures at different hydrate masses and  $Da$  numbers. The Hydrate crystal in (a) is very incompact. As the  $Da$  number decreases, it becomes more compact. This result is consistent with that of the MPDLA simulation of solidification structures of alloy melt, in which the morphology transforms from open cluster-type structures, via coral-type structures, to compact structures as the process changes from diffusion-controlled to interface kinetics-controlled [3]. In addition, the Hydrate shape in case (d) is a fairly round shape. This indicates that our model is free of lattice grid effects.

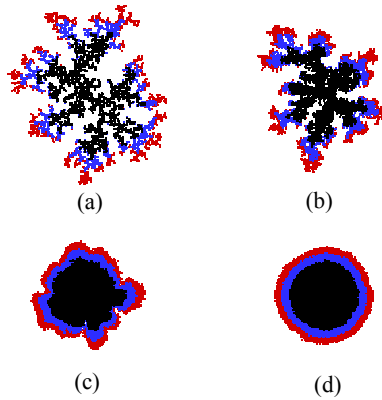


Figure 3: Hydrate structures at different hydrate masses and  $Da$  numbers.

Table 1 Fractal dimension values

$Da$	2	48	96	150	600
$D_f$	$2.002 \pm 0.001$	$1.95 \pm 0.01$	$1.80 \pm 0.02$	$1.77 \pm 0.02$	$1.75 \pm 0.02$

Since both reaction rate constant and diffusivity depend on the gas type, the formation of different gas hydrates may fall into different categories. Therefore, its impact on the medium properties may be very different. For example, the formation of type (a) hydrate in a medium may result in a larger decrease of permeability of the medium than the formation of type (d) hydrate. The approximate  $Da$  numbers calculated based on the data provided by Malegaonkar et al [17] are about one and two orders of magnitude smaller than unity for carbon dioxide and methane hydrate formation, respectively. Therefore, both hydrates are compact and have a round shape according to our simulations. This is consistent with the assumption in their model that the particles are spherical [1,16,17].

Table 1 shows approximate fractal dimension values ( $D_f$ ) for the hydrate structure at different  $Da$  numbers. As can be seen,  $D_f$  decreases from about 2 (the Euclidian dimension of a circle) to 1.75 (only 2.3% greater than 1.71, the fractal dimension of a DLA structure [18]) as  $Da$  number increases from 2 to 600.

Figure 4 shows dependence of the square of the radius of gyration on  $Da$  number. The number of particles (hydrate mass) is 3000 and saturation=1.2. Symbols in different colors are from different realizations. The radius of gyration indicates the compactness of the hydrate [18]. It is clear that as the  $Da$  number increases, the radius increases too, showing a decrease of the compactness of the hydrate structure. The radius has two asymptotic values, one at a very small and one at a very large  $Da$  number, and it varies according to a power law at  $Da$  number values in between.

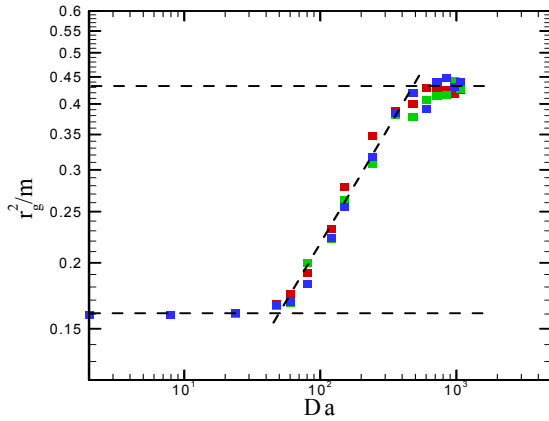


Figure 4: Dependence of the square of the radius of gyration on  $Da$  number. The number of particles (hydrate mass) is 3000 and saturation=1.2. Symbols in different colors are from different realizations.

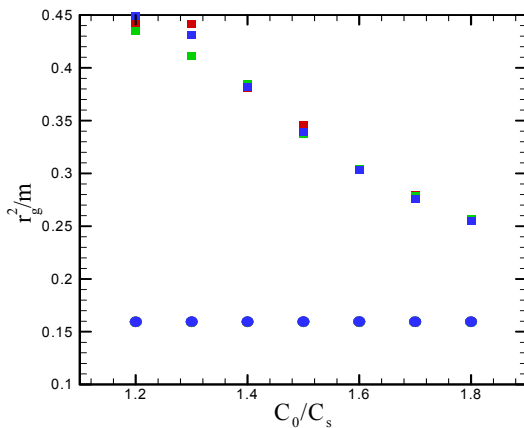


Figure 5: Dependence of the square of the radius of gyration on saturation at equilibrium state. Symbols in different colors are from different realizations.

Figure 5 shows the dependence of the square of the radius of gyration of the hydrate on the saturation for different  $Da$  numbers. It is clear that at a large  $Da$  number, the radius decreases as the saturation increases. This is so because there is only one initial nucleus in the system and hydrate formation can only occur at the liquid-hydrate interface. Therefore, a high degree of supersaturation makes it easier for the solute to transport to the interface and hence the process is more like a reaction-controlled one. The effect of saturation becomes less important at very small  $Da$  number because the

process is already reaction-controlled. Since this observation is relative to each single nucleus, it may be different from experimental observations, where the supersaturation may cause the formation of multiple nuclei in the system, hydrate may grow from these nuclei anywhere in the system, resulting in incompact overall hydrate structures.

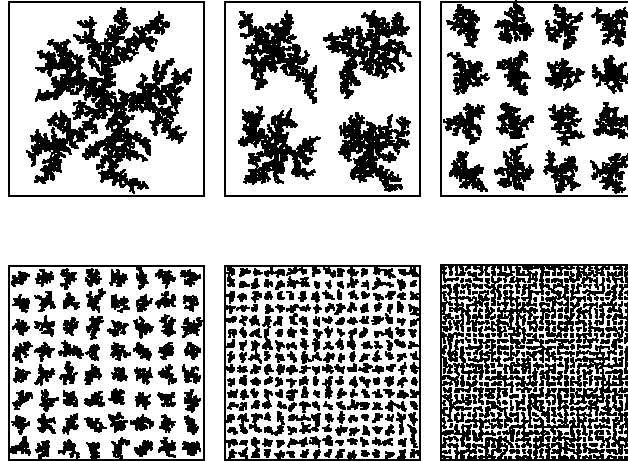


Figure 6: Hydrate structures at equilibrium state for initial saturation 1.2. The number of initial nuclei is: (a) 1; (b) 4; (c) 16; (d) 64; (e) 256; (f) 1024.

To demonstrate this, we have performed a set of simulations of hydrate formation from multiple initial nuclei uniformly distributed in the system. Figure 6 shows hydrate structures at equilibrium state for initial saturation 1.2 and different number of initial nuclei. As the number of initial nuclei increases, the hydrate clusters distribute more widely in the entire domain and hence are less compact. As the number increases further, the interaction between hydrate clusters from different nuclei tends to make the clusters more compact.

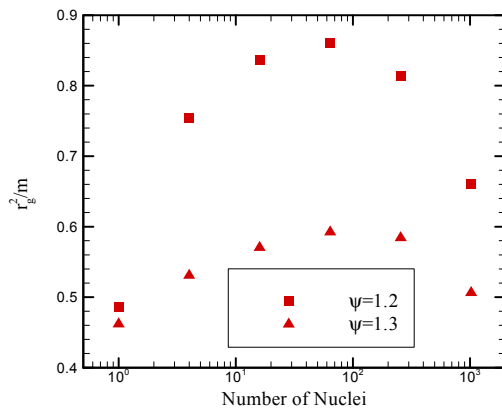


Figure 7: Dependence of the square of the radius of gyration on the number of initial nuclei at two different saturations.

Figure 7 shows dependence of the square of the radius of gyration on the number of initial nuclei at two different saturations. The radius of gyration of the cluster from a single nucleus at a lower saturation is smaller than that of the clusters from multiple nuclei and at a higher saturation. This implies

that the hydrate clusters of a system with higher saturation may be less compact than those of a system with lower saturation because the higher saturation may cause the formation of more initial nuclei in the system.

We also have some preliminary results for hydrate formation with fluid flow. Initially, the solution is saturated and there is no hydrate formation. At time zero, a single nucleus is introduced at the center of the domain and a pressure gradient is applied along the horizontal direction, and the saturation of the inflowing fluid is fixed at 1.2. In addition to saturation and Damkohler number, there is another control parameter, Plect number ( $Pe$ , the ratio of convection to diffusion).

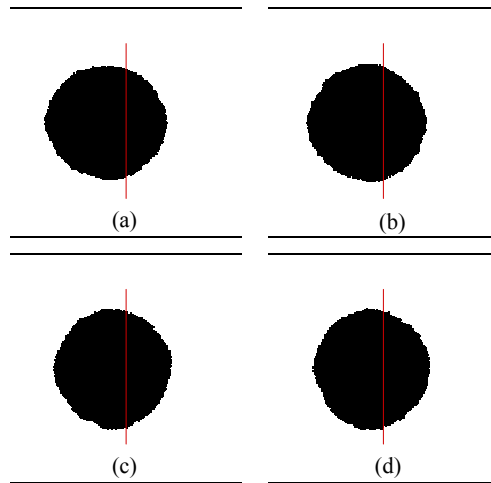


Figure 8: Hydrate structures at  $Da=5.77$  and at different  $Pe$  numbers. Hydrate mass=8000 (a)  $Pe=3.42$ ; (b)  $Pe=68.38$ ; (c)  $Pe=136.75$ ; (d)  $Pe=205.13$ .

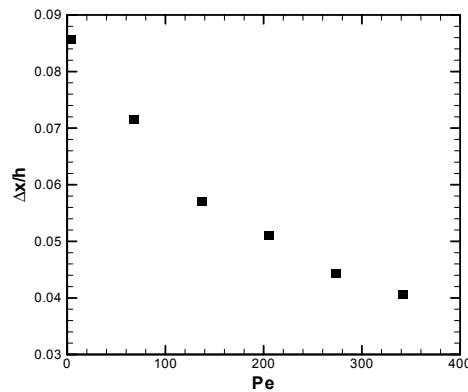


Figure 9: Shift of the hydrate crystal center towards the upstream at different  $Pe$  numbers:  $Da=5.77$ .

Figure 8 shows hydrate structures at  $Da=5.77$  and at different  $Pe$  numbers. The red vertical line indicates the horizontal position of the initial nucleus. Since the  $Da$  number is small and the process is reaction-controlled,  $Pe$  number does not have much impact on the shape of the hydrate crystal. As shown

in figure 8, they all have a round shape. However, it does change the position of the cluster center. The center of the hydrate crystal will shift towards the upstream, because the solute needed for the hydrate formation is provided by the supersaturated solution from the entrance. Figure 9 shows the shift of the hydrate crystal center towards the upstream at different  $Pe$  numbers. The larger the  $Pe$  number, the smaller the shift.

## Conclusions

We have simulated the hydrate crystal growth during CO<sub>2</sub> sequestration using a lattice Boltzmann method. We consider a first-order kinetic model for hydrate formation and the effect of temperature and pressure can be taken into account through diffusivity and reaction rate constant. We find that hydrate structure becomes less compact and its fractal dimension decreases approaching the DLA value as the  $Da$  number increases. At high  $Da$  number, hydrate growth from a single nucleus becomes more compact with increased super-saturation of the initial solution. The center of the hydrate crystal will shift towards upstream and the smaller the  $Pe$  number, the larger the shift. Anisotropic growth can be achieved by varying the probability ratio between the growth in the direction of nearest and diagonal nodes.

## Acknowledgements

This work was supported by LDRD/DR Project No. 20030059, sponsored by Los Alamos National Laboratory, which is operated by University of California for the U. S. Department of Energy.

## References

- [1] Bishnoi P. R. and Natarajan, V. 1996 Formation and decomposition of gas hydrates, *Fluid Phase Equil.* 117, 168.
- [2] Langer, J. S. 1980 Instabilities and pattern formation in crystal growth, *Rev. Mod. Phys.* 52, 1.
- [3] Das A. and Mittemeijer, E. J. 2001 A Monte Carlo simulation of solidification structures of binary alloys, *Philo. Magaz. A* 81, 2725.
- [4] Miller, W., Succi, S., and Mansutti, D. 2001 Lattice Boltzmann model for anisotropic liquid-solid phase transition, *Phys. Rev. Lett.* 86, 3578.
- [5] Chen, S. and Doolen, G. D. 1998 Lattice Boltzmann method for fluid flows. *Annu. Rev. Fluid Mech.* 30, 329.
- [6] Kang, Q., Zhang, D., Chen, S., and He, X. 2002 Lattice Boltzmann simulation of chemical dissolution in porous media, *Phys. Rev. E* 65, 036318.

- [7] Kang, Q., Zhang, D., and Chen, S. 2003 Simulation of dissolution and precipitation in porous media, *J. Geophys. Res.* 108, 2505.
- [8] Kang, Q., Tsimpanogiannis, I. N., Zhang, D., and Lichtner, P. C. 2004 Pore-scale studies of oceanic CO<sub>2</sub> sequestration, *Fuel Proc. Tech.* Submitted.
- [9] Kang, Q., Zhang, D., and Chen, S. 2002 Displacement of a two-dimensional immiscible droplet in a channel, *Phys. Fluids* 14, 3203.
- [10] Kang, Q., Zhang, D., and Chen, S. 2004 Immiscible displacement in a channel: Simulations of fingering in two dimensions, *Adv. Water Resour.* 27, 13.
- [11] Kang, Q., Zhang, D., and Chen, S. 2004 Displacement of a three-dimensional immiscible droplet in a duct, *J. Fluid Mech.* In revision.
- [12] Kang, Q., Zhang, D., and Chen, S. 2002 Unified lattice Boltzmann method for flow in multiscale porous media, *Phys. Rev. E* 66, 056307.
- [13] Zhang, D. and Kang, Q. 2004 Pore scale simulation of solute transport in fractured porous media, *Geophys. Res. Lett.* in revision.
- [14] Kang, Q., Zhang, D., Lichtner, P. C., and Tsimpanogiannis, I. N. 2004 Lattice Boltzmann model for hydrate crystal growth from supersaturated solution, *Phys. Rev. Lett.* Submitted.
- [15] Tohidi, B., Anderson, R., Clennell, M. B., Burgass, R. W. and Biderkab, A. B. 2001 Visual observation of gas-hydrate and dissociation in synthetic porous media by means of glass micromodels, *Geology* 29, 867.
- [16] Englezos, P., Kalogerakis, N., Dholabhai, P. D., and Bishnoi, P. R. 1987 Kinetics of gas hydrate formation from mixtures of methane and ethane, *Chem. Eng. Sci.* 42, 2647.
- [17] Malegaonkar, M. B., Dholabhai, P. D., and Bishnoi, P. R. 1997 Kinetics of carbon dioxide and methane hydrate formation, *Canadian J. Chem. Eng.* 75, 1090.
- [18] Feder, J. 1988 *Fractals*, Plenum Press, New York and London.